Journal of Manufacturing Processes 84 (2022) 871–885

Contents lists available at ScienceDirect

Journal of Manufacturing Processes

journal homepage: www.elsevier.com/locate/manpro

Turning of titanium alloy with PCD tool and high-pressure cooling

Petr Masek [a,*], Jan Maly [a], Pavel Zeman [a], Petr Heinrich [b], Nageswaran Tamil Alagan [c]

[a] Department of Production Machines and Equipment (RCMT), Faculty of Mechanical Engineering, Czech Technical University in Prague, Czech Republic
[b] Kovosvit MAS Machine Tools, Sezimovo Usti, Czech Republic
[c] Innovation and Technology, Extrusion Europe, Norsk Hydro, Norway

ARTICLE INFO

Keywords:
High-pressure cooling
PCD tool
Tool wear
Ti6Al4V

ABSTRACT

Titanium alloys are difficult to cut materials due to their low thermal conductivity, which leads to intensive tool wear. The general issue is finding the best combination of cutting tool material and cutting conditions to achieve high productivity. This study used PCD cutting tool material in combination with high-pressure cooling (HPC). The main task was to find the most suitable HPC mode (various HPC settings on the rake and flank faces of the cutting tool) and intensity to reduce tool wear at a high cutting speed. Tool wear, chips, and forces were measured, and surface quality was evaluated to gain an understanding of the machining process under these particular conditions. An ANOVA test was used to determine the significance of control factors such as tool life and HPC mode and intensity. The most suitable cutting speed was 300 m/min, where a limit spiral cutting length (SCL) of 3000 m was achieved. Setting the HPC mode revealed the necessity of using the HPC on the rake face. However, the HPC on the flank face further decreased tool wear. HPC intensity should be chosen based on knowledge of the cutting process. A very intense HPC above 140 bars can lead to mechanical damage to the cutting edge or unmachined surface by chip blasting but using a 60-bar HPC can reduce tool wear similarly, without causing further damage to the cutting edge.

1. Introduction

A significant challenge in machining titanium (Ti) alloys is dissipating the heat generated from the cutting zone due to the material's low thermal conductivity properties (~6.7 Wm^{-1} K^{-1}). Coolants have been widely used as a medium to reduce the heat from the cutting zone, leading to a significant increase in tool life. One of the most commonly used alloys within the family of Heat Resistant Super Alloys (HRSA) is Ti6Al4V, which is used in the aircraft and medical industries due to its ability to retain its mechanical and thermal properties at elevated temperatures and its corrosion resistance properties.

The industrial standard for machining titanium alloys is coated cemented carbides due to their abrasive wear resistance and breakage resistance, despite their positive tool geometry. However, further increases in cutting speed due to increased productivity are very limited even when coolant is used. Researchers and some industries have begun looking for an alternative to improve the machinability of Ti alloys. Due to advances in cutting tool materials aimed at improving the robustness of the manufacturing process, ultra-hard cutting materials are beginning to be used extensively and have increased cutting performance compared to cemented carbides under certain cutting conditions. This group of tools includes tools made of polycrystalline cubic boron nitride (PCBN) and polycrystalline diamond (PCD) [1–3]. These cutting materials have high hardness and thermal conductivity properties in comparison to cemented carbides. Sun et al. [4] compared PCBN and PCD tools and found that PCD had a longer tool life. However, the low temperature of the diamond degradation and the strong affinity of carbon to titanium limit their use; the temperature is ~800 °C. However, using coolant in combination with PCD tools has demonstrated the ability to extend cutting tool potential.

Choosing a suitable PCD is important in terms of increasing tool life. Grain size is one of the basic parameters which affect tool life. Several studies have presented the influence of PCD grain size in the machining of titanium alloys [5–8]. The cobalt-to-diamond ratio seems to be of equal importance. The grain size significantly affects the mechanical properties of the cutting edge (coarse grains tend to break off). The effect of grain size can influence the morphology of the machined surface, as discussed in [5]. The thermal conductivity of PCD made from coarse grains is higher than that of fine-grained PCD, e.g. the thermal conductivity for 2 μm is 239 W/mK and for 10 μm it is 456 W/mK, as

* Corresponding author.
E-mail address: p.masek@rcmt.cvut.cz (P. Masek).

https://doi.org/10.1016/j.jmapro.2022.10.034
Received 15 July 2022; Received in revised form 11 October 2022; Accepted 12 October 2022
Available online 2 November 2022

reported by Li [7]. The research results showed that coolant-assisted machining with a PCD tool with a grain size of 2 μm was superior due to the high abrasive resistance and higher thermal conductivity when titanium aluminides were machined. Further, the study identified a shorter tool life when the grain size was between 7 and 10 μm [9]. The main cause of PCD tool wear during the machining of Ti6Al4V was a combination of adhesion, abrasion, and attrition [10]. Sadik et al. explained the progression of crater wear on the rake by TiC formation (diffusion) and PCD graphitization [11].

The coolant plays an important role in dissipating the heat energy from the cutting zone and extending tool life. Research into high-pressure cooling dates back to the early 1950s when Pigott and Colwell [12] built a high-pressure cooling system that was able to increase tool life up to 8 times compared to flood cooling when machining various types of steel. Isolated attempts to investigate the potential of high-pressure cooling followed, and in the late 1970s Sandvik Coromant introduced the Jet-Break™ system, primarily for machining titanium alloys in the aerospace industry. This system made it possible to increase machining productivity by increasing cutting speeds [13]. The greater number of publications focusing on high-pressure cooling of titanium alloys was published in the 1990s, when high pressures [14], sometimes approaching waterjet cutting pressures [15], were experimented with, and in the early 2000s, when pressures up to 30 MPa were tested [16–19]. These publications were focused on understanding the effect of HPC on chip formation, wear mechanisms, and tool-workpiece interaction. López de Lacalle et al. [16] presented a doubled chip flow and 50 % reduction of machining time when HPC was used in comparison to dry machining of titanium alloy. There are many usable cooling environments suitable for titanium alloy machining. Benedicto et al. compared various types of water-based cooling instead of HPC [20] and found water-based MWF with synthetic esters to be the most suitable. Hosokawa et al. tested the effect of HPC from the rake and flank directions as well as a rake-flank combination. They found the combination to be the most effective option for decreasing the temperature in the cut and reducing the chip volume [21]. However, HPC reduces chip volume, but its use can be environmentally disadvantageous [22]. The environmental impact of cryogenic cooling was assessed to be smaller compared to wet cooling and even more effective in terms of tool life in combination with MQL by Pereira et al. [23]. Many recent articles focus on the cryogenic cooling of titanium alloy, e.g. Yang et al. [24], Zavada-Tomkievicz et al. [25] or Airao et al. [26] and Khanna et al. [27], with a significant reduction of heat in the cutting zone and extension of tool life. Another approach to decreasing the temperature in the cutting zone and tool wear without using wet cooling is to decrease the friction between the formed chip and the cutting tool, as presented in [28,29]. Despite research into alternative heat removal options, HPC is still advantageous due to its high heat removal capability and positive effect on chip formation. In addition, the cut zone can be affected differently by varying the cooling intensity.

The correct cooling choice when machining titanium alloys with a PCD tool is very important and several papers have investigated this topic. da Silva et al. [10] investigated the influence of different methods of cutting zone cooling, including dry machining, minimum quantity lubrication (MQL), and high pressure coolant during tool wear the most. The influence of HPC on PCD tool life was presented by da Silva et al. in a previous study [30], which investigated the influence of the pressure intensity dependent on the cutting speed. Increasing pressure had an influence on tool life only up to a cutting speed of 200 m/min. HPC did not show any effect above this cutting speed. Çolak [31] studied the influence of HPC during the machining of titanium alloy using cemented carbide. He experimentally proved that HPC had an influence of up to 300 bars. In another paper where the selected range of HPC was 50 to 250, bar it was found that HPC above 100 bar does not have a positive effect on cemented carbide tool life [32]. Wada found that HPC had a positive influence on chip breakage and tool life [33]. Palanisamy et al. found smaller chips and three-fold higher tool life when HPC 90 bar was used for cooling alloy Ti6Al4V with a cemented carbide insert compared to standard cooling [34]. Flood cooling or MQL was found to have only a minor effect when Ti-5553 alloy was machined at high cutting speeds in terms of the cutting forces, chip thickness, dimensional accuracy, and microhardness measurements. On the other hand, HPC had a positive effect [35]. Rao et al. used MQL for the cooling of the cutting zone using small holes drilled on the rake face of the PCD tool. They achieved increased tool life compared to conventional MQL [36]. In a further study, C. M. Rao compared this modified PCD with a similarly modified PCBN where MQL did not have such a positive effect under the selected cutting conditions [37]. Sales et al. compared LN_2, flood and a combination of LN_2 and flood with MQL. They were able to reduce the resulting power through a combination of coolant strategies. In their study, they described the PCD tool wear mechanism for flood and LN_2 coolants [38]. Ravenkar et al. focused on the effect of dry, flood and MQL cooling on surface quality when machining titanium alloy with a PCD cutting tool [39]. They found that MQL is essential for better surface quality. They recommended a low cutting speed of 50 m/min and a feed per revolution of 0.25 mm. Mia et al. [40] recommended a high cutting speed of 156 m/min and a small feed per revolution of 0.12 mm when HPC is applied to decrease surface roughness.

Titanium alloy machinability may be improved by machining under certain cutting conditions with a beta transition temperature [41]. A change in cutting speed has a direct relation to the temperature in the cutting speed. Thus, an increase in cutting speed due to an increase in productivity leads to a rapid decrease in tool life. One research paper identified and recommended limiting the cutting speed to a range of 50 to 110 m/min for cemented carbide cutting tools when machining Ti6Al4V [8]. Interesting results were found when using high-pressure coolant in combination with PCD tools. It was possible to increase the cutting speed above 100 m/min. In particular, a range of cutting speeds from 160 to 250 m/min was widely investigated and recommended for use in production as the normal range. A cutting range of 80 to 150 m/min was used for flood cooling and dry machining in ref. [5]. Wada [33] was able to push the limits of PCD tools in a cutting speed range of 450 to 700 m/min with HPC in a range of 7 to 20 MPa. Other authors used cutting speeds ranging from 175 to 250 m/min and HPC from 7 to 20.3 m/min [30]. Ezugwu et al. used the same cutting speed range and HPC from 11 to 20.3 MPa [42]. The starting cutting conditions for the experimental work described in the present paper were set based on these studies.

The PCD tools are extremely hard cutting material, but it is also very brittle and with their use have a thermal limitation. Based on a study of the literature and the author's previous research in machining titanium with ultra-hard tools, the following research gaps were identified. PCD cutting tools are not commonly used for machining titanium alloys and still require knowledge of *know-how* to use PCD for titanium machining in combination with high-pressure coolant. The novelty of this work stated in three aspects:

- Firstly, flank cooling is not a commonly researched topic. Although the tertiary shear zone is of high importance for temperature control. Especially in machining heat-resistant superalloys.
- Secondly compared to most of the published work on the cooling effect in titanium turning, this work focuses on PCD tools instead of carbide tools. In addition, it assesses the effect of pressure intensity and the suitability of using dual HPC from both face and rake.
- Thirdly, the effect of change in HPC when turning Ti6Al4V alloy with a PCD tool was considered not only in terms of tool wear but also in terms of forces, chip formation and quality of the machined surface to better understand the effect of HPC on the cutting process.

2. Experimental setup

2.1. Workpiece and cutting tool

The workpiece material was a wrought bar of annealed Ti6Al4V; see mechanical properties in Table 1. The diameter of the bar was 250 mm and the length of 990 mm. The chemical composition of the Ti6Al4V used for the experimental investigation was made by the producer of the workpiece and was adopted from the quality certificate; see Table 2. The results on the top were measured near the surface and the results on the bottom were measured near the middle of the round bar.

A PCD cutting tool was used for the experimental investigation. An RCMX 120400 indexable insert without chipbreaker and a negative facet was chosen and CMT302 PCD was soldered to it. This multi-modal PCD contained diamond particles ranging from 2 to 30 μm in size. The high content of the diamond particles on the cutting edge was ensured by laser cutting geometry. The measured geometry of the cutting tool was rake angle 0.05° ± 0.24°, flank angle 8.66° ± 0.33° and cutting-edge radius 2.53 μm ± 0.28 μm. A special tool holder with internal delivery of high-pressure coolant to the rake and flank faces of the cutting tool was used in this application.

2.2. Machine tool and measuring methods

A SP430Y turning centre with fluent cutting speed regulation was used in the experimental investigation. The maximum spindle revolution was 3800 1/min and the maximum spindle power is 28 kW. The cutting speed was kept constant for each workpiece's diameter. The experimental setup in the machine tool is shown in Fig. 1.

A special device for splitting and measuring the HPC flow delivered by the high-pressure coolant system was designed for the needs of the experiment. Each branch of HPC could be regulated separately and flow and pressure measurements were possible. One of the branches delivered HPC to the flank face and the other to the rake face of the cutting tool; see Fig. 3b.

Cutting tool wear was measured at predetermined times. Flank wear as well as rake wear were measured according to ISO 3685: 1993, taking into account the characteristics of the round indexable insert. Flank wear was measured in the tool corner (VB_c) and the crater back (KB) (Fig. 2). A Keyence VHX-7000 digital microscope with 4 K resolution was used to photograph and measure cutting tool wear. Tool wear was measured after every 2 min in the cut. The limit spiral cutting length (SCL) was determined as 3000 m.

The forces were measured using a Kistler 9257B multi-component dynamometer. This 3-axis measuring device was connected to a LabAmp 5167Ax0 high-sampling data acquisition device for generic piezoelectric measurements by Kistler. All recorded forces were evaluated in Kistler Dynoware 3.2 software. The cutting force F_c, the feed force F_f and the passive force F_p were measured (Fig. 3a). The coordinate systems of the machine tool and dynamometer were precisely aligned. The forces were measured at the beginning of each experimental run when the cutting edge did not have any tool wear.

The chips were collected in a woven tarpaulin during machining. The chips were photographed with a Canon EOS 505D digital camera to determine the forms of the chip according to the ISO 3685: 1993 standard. The selected basic chip dimensions were measured with a LIM digital microscope. Curl radius (r) (Fig. 4a) and chip thickness (t) (Fig. 4b) were measured in this study. The thicker sides of the chip were measured.

Surface roughness was measured according to the DIN EN ISO 4288: 1998 standard. A Surtronic 3+ portable self-contained instrument for surface texture measurement was used to determine Ra parameters. A Gaussian filter and cut-off of 0.8 mm were set for all measurements.

Table 1
Basic mechanical properties of Ti6Al4V.

Property	Symbol	Unit	Value
Tensile strength	*Rm*	MPa	965
Yield strength 0.2 %	Rp_{02}	MPa	867
Elongation	*A*	%	14.5
Reduction of area	*Z*	%	31

2.3. Design of experiment

The experimental design consisted of 3 separate blocks. The first block served as a preliminary experiment to determine the appropriate cutting speed. The three-level design of the experiment included cutting speeds of 200, 300 and 400 m/min. The other cutting parameters remained constant. The feed per revolution (f_n) was 0.2 mm, the axial depth of cut (a_p) was 0.3 mm and the selected HPC was 80 bar - the same pressure for both the rake and the flank surfaces of the cutting tool (Table 3).

Based on the results of the preliminary experiment, only one cutting speed was selected for the second and third blocks of the experiment. The second block was designed to determine the effect of HPC in the flank and rake directions, both separately and together. The measured responses were cutting forces, tool wear, surface roughness and chip formation (Table 4).

The third block of the experiment focused on the increase of HPC intensity and its effects on cutting forces, tool wear, surface roughness and chip formation. The HPC was the same for both the rake and the flank faces (Table 5).

A full factorial experimental design with three replications was adopted for all three experiments. Analysis of variance was used as a statistical approach to determine the significance of the HPC effect on the measured responses.

3. Results and discussion

3.1. Test of cutting speed effect

This test focused on PCD tool wear under various cutting velocities. It was expected that low cutting speed should have the smallest tool wear after machining 3000 m of the cutting tool length. However, the test revealed a different tool wear result.

Machining under low cutting speed (v_c = 200 m/min) and HPC (80 bar on rake, 80 bar on flank) caused a brittle fracture of the cutting edge in most cases (Fig. 5). An excessively low temperature in the cut most likely meant greater susceptibility to a brittle fracture of the cutting edge under these cutting conditions. Chipping and then tool breakage could be observed on the cutting edge. However, there was one replication of this particular run where no chipping was observed. Flank wear after reaching the SCL limit was only VB_c = 109 μm; for instance, flank wear was VB_c = 270 μm on average for v_c = 300 m/min. The other attempts to repeat this result failed and it was assumed that it was an accidental case. The temperature increased with cutting speed and at v_c = 300 m/min adhesion was more present. The HPC was not able to dissipate heat when v_c = 400 m/min was used and most likely the diamond graphitization temperature was exceeded in the wide area around the cutting edge. This could explain the rapid tool wear on the rake and flank faces near the cutting zone.

3.2. Testing of various HPC modes

This set of experiments focused on the effect of HPC on the rake face, flank face and both faces of the cutting tool in comparison to machining without HPC. The cutting forces, tool wear and chips were measured.

3.2.1. Cutting forces

The coolant flows from the nozzles' induced force under high pressure, which was measurable by a dynamometer, and this force affected

Table 2
Chemical composition of Ti6Al4V.

[Weight %]	Al	V	Fe max	C max	O max	N max	H max	Y max	Ti
Result TOP	6.07	4.07	0.201	0.0115	0.169	0.0065	0.0031	<0.001	Bal.
Result BOT	6.11	4.02	0.171	0.0116	0.183	<0.0030	0.0031	<0.001	Bal.

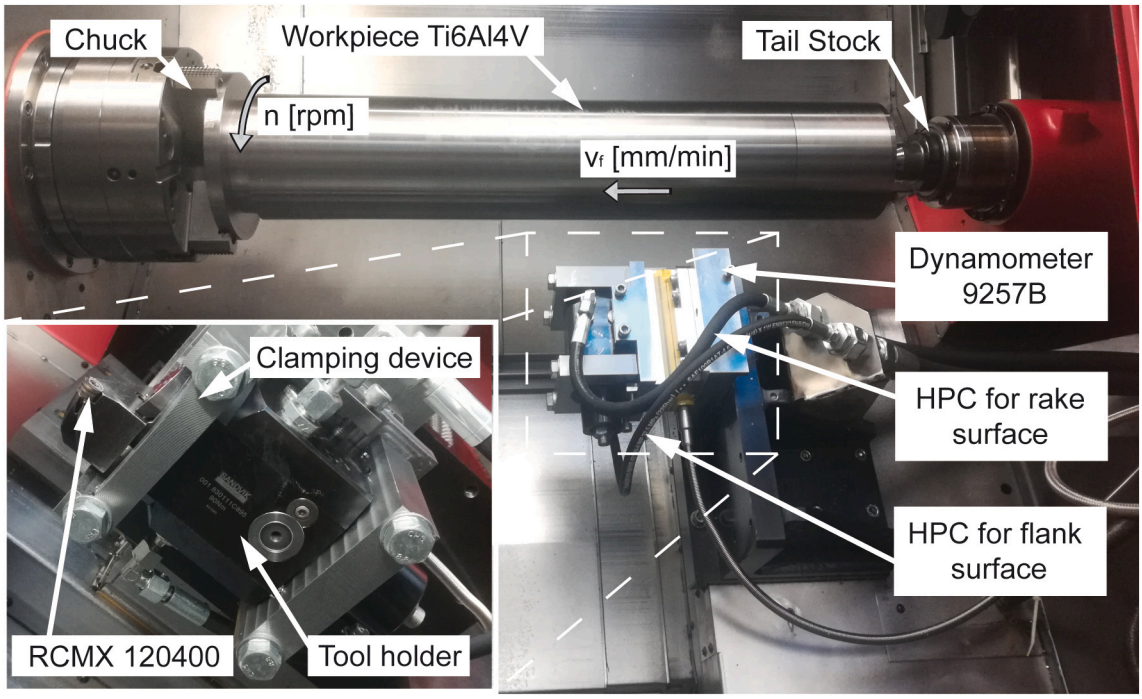

Fig. 1. Experimental setup placed in the SP430Y CNC lathe.

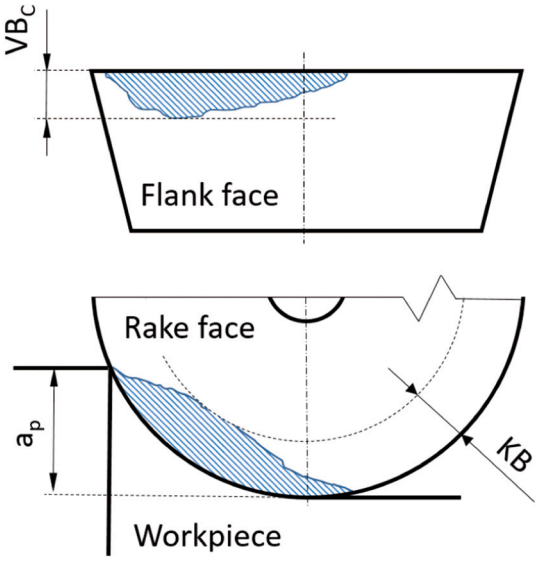

Fig. 2. Schema of round insert tool wear measurement.

the cutting process. The force effect of the coolant pressure on the tool's flank face was most pronounced on the X-axis of the dynamometer (in the tangential direction to the cutting speed). The HPC on the rake face acted the most on the *Z*-axis of the dynamometer (in the feed direction). The Y-axis (in the radial direction to the cutting speed) was loaded from both directions of the HPC, but slightly more from the rake direction (see Fig. 3a,b). The contribution of the HPC to the force in each direction is relatively significant and it had to be taken into account mainly when thin parts were machined (Fig. 6).

The cooling effect of the HPC on the force was evaluated with an ANOVA test. This test revealed that the HPC had a significant effect on the rake face in terms of F_f and F_p. At the significance level $\alpha = 0.05$, the HPC on the rake face significantly affected F_f and F_p (Tables 6 and 7). The influence of the HPC on the flank face was statistically insignificant at the selected significance level. The coefficient of determination was 88 % for the F_p model and 90 % for the F_f model. F_c could not be evaluated by the ANOVA test because the data were not normally distributed. The nonparametric Kruskal-Wallis test was used instead. According to the *p*-values for HPC on the rake (0.288) and on the flank (0.188), which were higher than the selected significance level $\alpha = 0.05$, the HPC on the flank and rake was statistically insignificant for the control factor F_c. This evaluation yielded several findings. Machining without coolant increased all of the measured force components. The HPC on the flank affected forces less than the HPC on the rake. This direction of the coolant did not affect chip formation, while this effect was observable for the direction of the rake.

HPC on the flank increased F_f and F_p and in the case of F_p, this would be an unfavourable situation for thin parts. When the HPC on the rake was turned off, the forces were significantly greater than when the HPC was turned on. The increase in pressure from 80 to 140 bar had a more significant effect on the forces in the rake direction than in the flank direction. F_f and F_p were reduced with the increasing HPC on the rake, as was F_c. However, the increasing HPC on the flank contributed to the reduction of F_c as well. The cutting force was reduced in the case of cooling from both directions, but only slightly (Fig. 7).

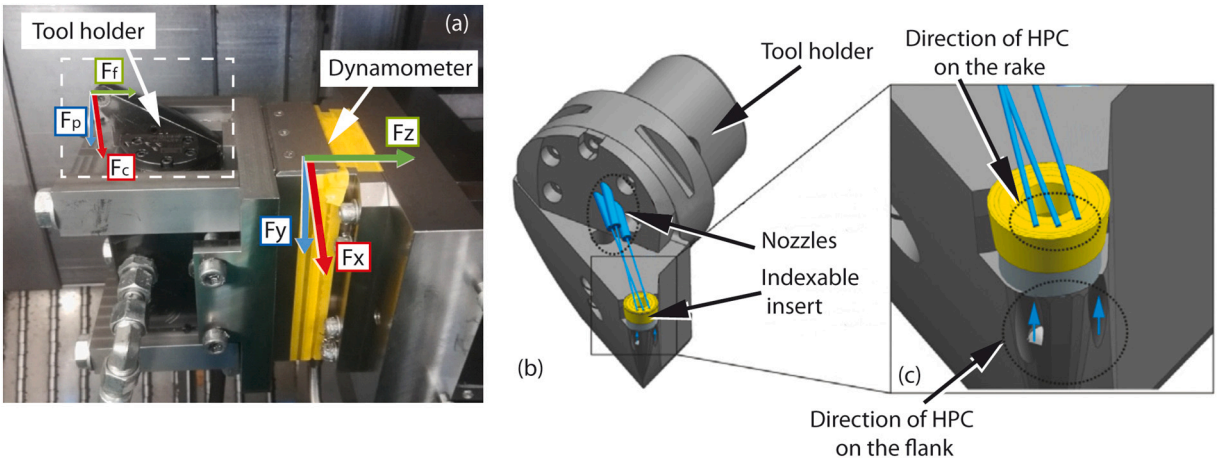

Fig. 3. Direction of the measured force components (a), Schematic view of the tool holder (b) and flow of HPC from nozzles (c) [43].

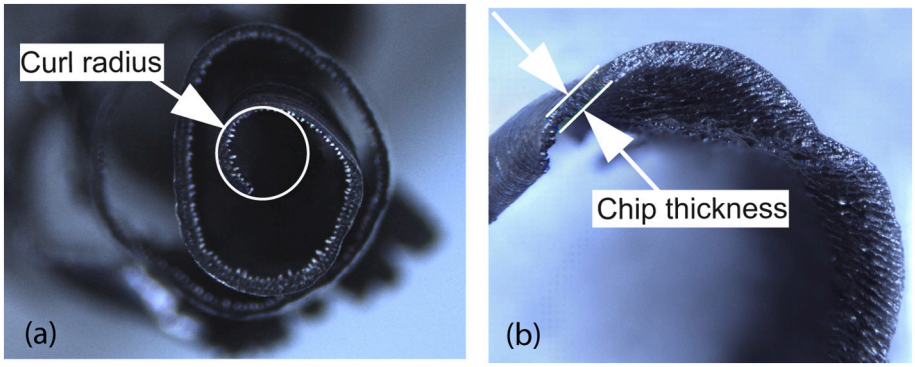

Fig. 4. Measurement of chip curl radius (a) and chip thickness (b).

Table 3
Design of experiment for testing cutting speed effect.

Parameter/factor			Level		
			1	2	3
Cutting speed	m/min	v_c	200	300	400
Feed per revolution	mm	f_n	0.2		
Axial depth of cut	mm	a_p	0.3		
HPC pressure (flank/rake)	bar	*HPC*	80		

Table 4
Design of experiment for testing various HPC modes.

Parameter/factor			Level		
			1	2	3
HPC on flank	bar	*HPC-f*	0	80	140
HPC on rake	bar	*HPC-r*	0	80	140
Feed per revolution	mm	f_n	0.2		
Axial depth of cut	mm	a_p	0.3		
Cutting speed	m/min	v_c	300 m/min (from preliminary tests)		

3.2.2. Tool wear

Measurement of tool wear below HPC 0/0 (0 bar on the edge and 0 bar on the side) was excluded from the evaluation. Under these coolant conditions, rapid tool wear was observed after 30 s of the cut. The massive loss of material from the cutting edge and increasing forces caused a total failure after 60 s of the cut. The main sign of tool wear was the burning of the cutting edge; see Fig. 8. We can assume that the limit temperature for PCD was exceeded for the cutting speed of 300 m/min.

Table 5
Design of experiment for testing HPC intensity.

Parameter/ factor			Level						
			1	2	3	4	5	6	7
HPC pressure (flank/rake)	bar	*HPC*	40	60	80	100	120	140	160
Feed per revolution	mm	f_n	0.2						
Axial depth of cut	mm	a_p	0.3						
Cutting speed	m/min	v_c	300 m/min (from preliminary tests)						

Sun et al. measured temperature at approximately 480 °C for a similar workpiece and cutting tool combination (far below the PCD limit temperature of ~800 °C) [4]. Nevertheless, in Sun's study, the cutting speed was 3 times lower and feed per revolution 2 times lower than the cutting speed and feed per revolution in this study. The exceeding of the PCD limit temperature may be predicted based on Sun's measurement approximations. This also explains the long cutting tool life under dry machining measured by Shalaby and Veldhuis for a cutting speed of 150 m/min, where the limit temperature was not reached [2].

In terms of cutting tool wear, the cooling was insufficient without the use of HPC on the rake. The cutting edge showed rapid degradation of the PCD material over time and was not able to machine after 8 min in a cut. The high temperature concentrated on the cutting edge caused destructive tool wear (crater wear from the cutting edge); see (Fig. 10 (c)). The HPC on the flank helped mainly with the cooling of the third deformation zone between the flank surface of the PCD and the

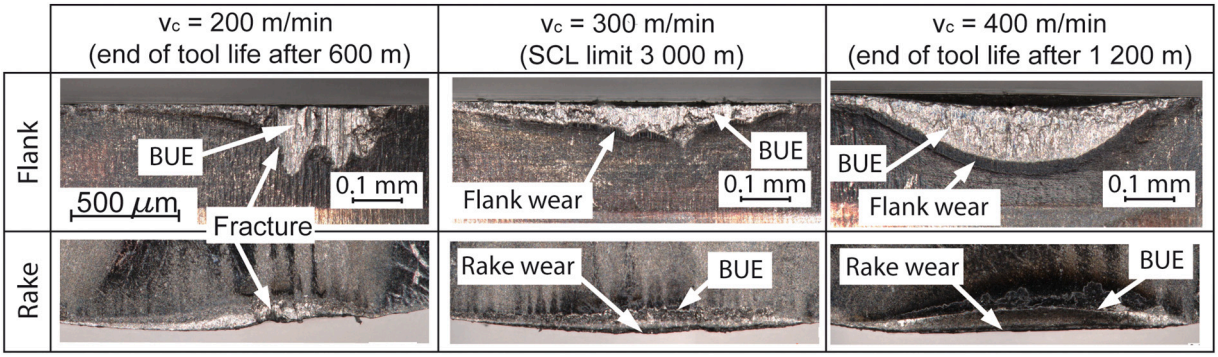

Fig. 5. Tool wear comparison for tested cutting speeds at HPC 80 bar on the rake and flank surfaces at the end of tool life (or after reaching the SCL limit).

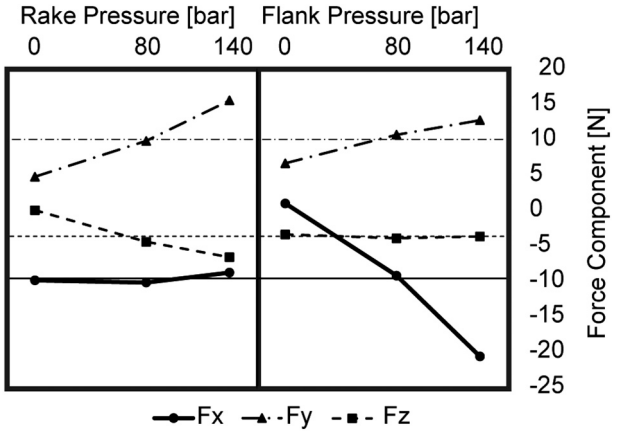

Fig. 6. Main effect plot for force effect of HPC.

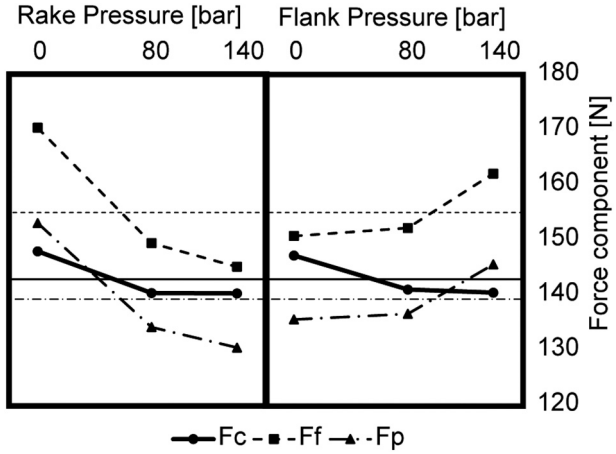

Fig. 7. Main effect plot for coolant effect of HPC on force components

Table 6
ANOVA table of results for feed force F_f.

Source	DF	Adj SS	Adj MS	F-value	*p*-Value
HPC on flank	2	227.9	113.93	3.2	0.148
HPC on rake	2	1093.4	546.68	15.36	0.013
Error	4	142.4	35.59		
Total	8	1463.6			

Table 7
ANOVA table of results for passive force F_p.

Source	DF	Adj SS	Adj MS	F-value	*p*-Value
HPC on flank	2	181.2	90.61	2.69	0.182
HPC on rake	2	882.1	441.07	13.11	0.018
Error	4	134.6	33.64		
Total	8	1197.9			

machined workpiece surface. The overheated and graphitized area on the PCD tool was reduced significantly with HPC from both directions. Without HPC on the flank, abrasive tool wear and chipping could be observed (Fig. 10(a)), as well as notch wear in the maximum depth of cut (Fig. 10(b)).

When using HPC from both directions, only a small displacement of the cutting edge was observed due to graphitization (Fig. 9). The HPC on the rake helped with chip formation. There was less contact between the chip and the rake surface of the PCD tool and the heat transition affected a smaller area on the rake surface. The crater zone was noticeably smaller when using HPC. Diamond graphitization can occur above 800 °C [3]. Microscopic ridges and caves may appear as a result of this local graphitization [44]. Tool wear observed during the tests was probably a combination of abrasion, adhesion (build-up edge – BUE), and diffusion wear. Due to the affinity of the carbon to the titanium, the diamond or graphite particles of the cutting edge are bound to the titanium and pluck out from the cutting edge due to the relative movement of the cutting tool and workpiece or chip. The diffusion starts at high temperatures and its contribution to wear was most likely small.

The ANOVA test was performed only up to 480 s of machining time because the three runs of the experiment did not reach the limit SCL. In addition, 0 bar HPC on the rake surface had to be excluded from the ANOVA test due to significantly different tool wear generation from other experimental data. These data strongly influenced the evaluation of all control factors.

At the significance level $\alpha = 0.05$, the null hypothesis was rejected for all control factors. All control factors were statistically significant. Based on the F-value, it was possible to estimate that HPC on the rake had the strongest effect on the VB_c change. The second strongest control factor was machining time. The use of HPC on the rake and increased pressure caused a reduction in the tool wear. Machining time increased flank wear. Flank wear increased slightly from 0 bar to 80 bar for HPC on the flank. After a further increase of HPC on the flank, VB_c decreased.

HPC on the rake and flank faces had almost the same effect as KB; see *p*-values in Tables 8 and 9. The null hypothesis of equality of variances for each of the control factors could not be rejected at the chosen significance level. The effect of HPC on the face and machining time was similar to VB_c. However, when using HPC on the flank, decreasing tool wear was measured from HPC 0 to 80 bar; see Fig. 11.

3.2.3. Chips

Chips were collected at the time of tool wear measurement. Tubular snarled chips were found only when HPC on the rake was turned off.

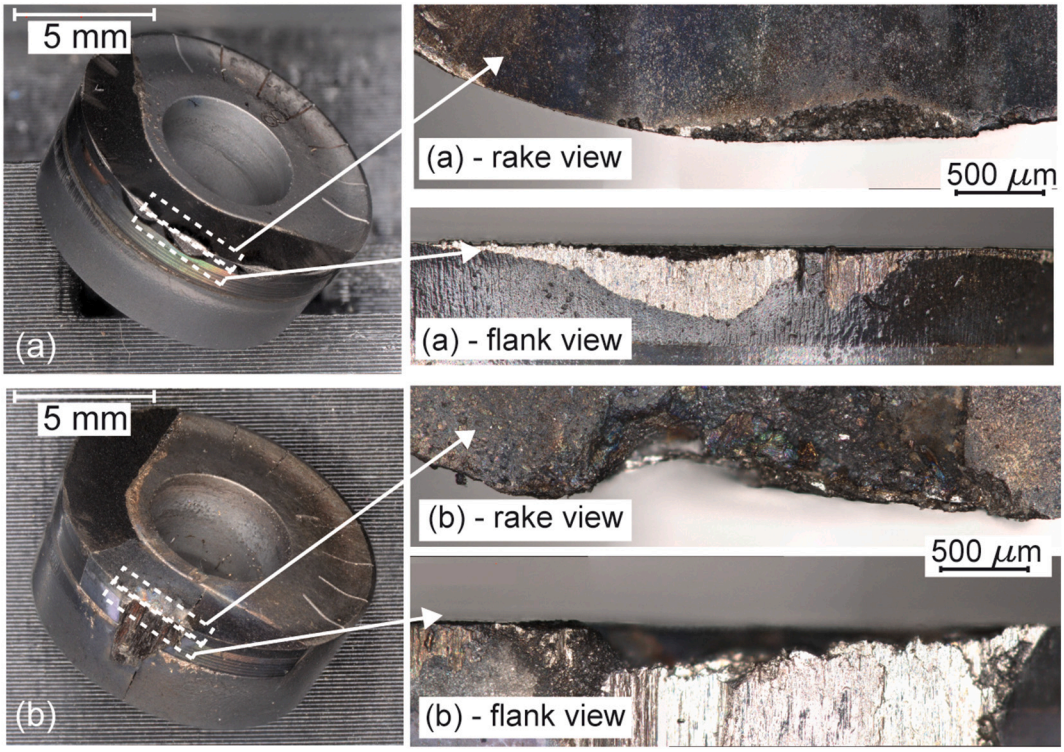

Fig. 8. Tool wear after 60 s under HPC 0/0: (a) after 30 s, (b) after 60 s.

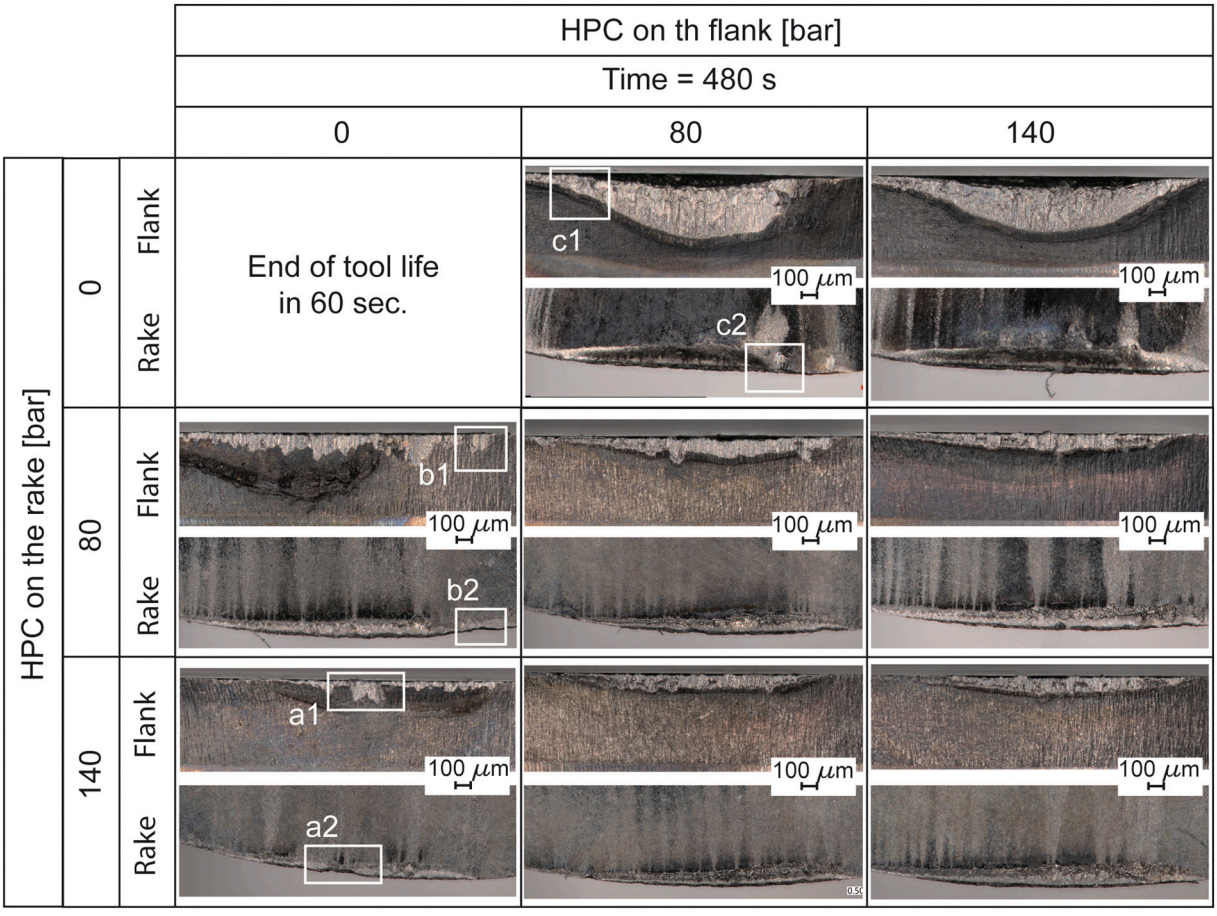

Fig. 9. Direct comparison of tool wear after 8 min in the cut for various HPC modes.

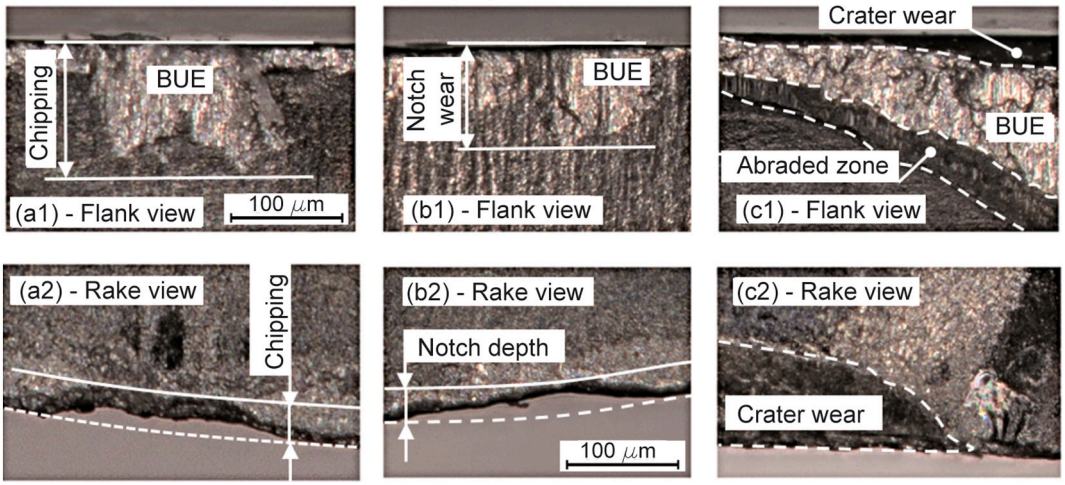

Fig. 10. Details from the direct comparison of tool wear after 8 min in the cut for: (a1) flank = 0 bar and (a2) HPC rake = 140 bar; (b1) flank = 0 bar and (b2) HPC rake = 80 bar; (c1) flank = 80 bar and (c2) HPC rake = 0 bar.

Table 8
ANOVA table of results for flank wear VB_c when various HPC modes were used.

Source	DF	Adj SS	Adj MS	F-value	*p*-Value
Time	3	9158	3052.60	44.61	0.000
HPC on flank	2	1030	515.20	7.53	0.005
HPC on rake	1	4998	4997.78	73.04	0.000
Error	17	1163	68.43		
Total	23	16349			

Table 9
ANOVA table of results for rake wear KB when various HPC modes were used.

Source	DF	Adj SS	Adj MS	F-value	P-Value
Time	3	1117.7	372.57	35.00	0.000
HPC on flank	2	1420.5	710.24	66.72	0.000
HPC on rake	1	693.4	693.37	65.13	0.000
Error	17	181.0	10.65		
Total	23	3412.6			

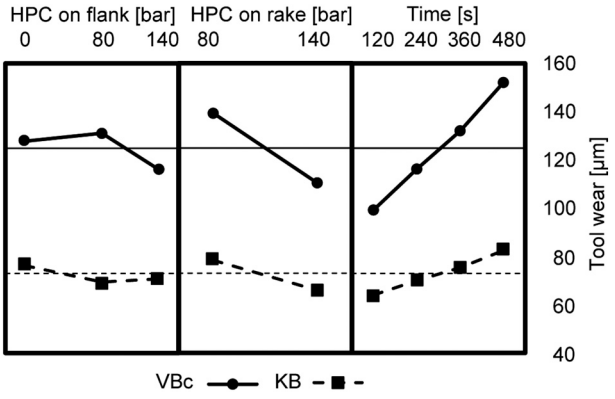

Fig. 11. Main effect plot for VB_c and KB when various HPC modes were used

After 8 min of cutting, the chips changed shape to ribbon snarled chips. The connection of segments identified as ribbon or tubular snarled chips can be explained by the increased tendency of chips to adhere under high temperatures in the cut, as described by Muhammad [45]. Ribbon chips were also observed when HPC was not used. Arc connected chips were formed using HPC 80 bar and higher on the rake surface. These chips appeared smaller when pressure was increased (Fig. 12). A similar effect of HPC on chip formation was presented by Hadzley et al. [46].

In the case of chip curl radius, ribbon chips and tubular chips were excluded from the ANOVA test. Ribbon chips showed no curl radius. Tubular chips exhibited a measurable curl, but their curl radius was several times higher than the arc chips. At the chosen significance level, the null hypothesis of equality of variances for the control factor of HPC on the rake can be rejected. That means that HPC on the rake actively affected the chip curl radius (Table 10). Neither HPC on the flank nor machining time had a statistically significant effect on chip curl radius. It was found that the chip curl radius decreased with HPC on the rake (Fig. 13). The coefficient of determination was 70 % for the estimated model due to the variability of the measured data.

Chip thickness was evaluated as statically independent of HPC on the flank and time according to the ANOVA test at the chosen significance level (Table 11). Chip thickness was significantly affected by HPC on the rake and chip thickness increased with HPC (Fig. 14). The coefficient of determination was 65 % in this case.

3.3. HPC intensity testing

3.3.1. Cutting forces

Measurements of the forces for increasing HPC intensity revealed that the cutting force is almost independent of increasing pressure. After reaching 100 bar, the cutting force does not respond to further increases in coolant pressure. The feed force and passive force increased non-linearly with coolant pressure (Fig. 15). The increase of the cutting force component was probably connected to the cooling of the cutting zone. Decreasing the temperature in the cutting zone increases the shear stress, as reported for instance in ref. [47]. Increasing the shear stress leads to the enlarging of the primary deformation zone and this manifested itself through the increasing cutting forces. The feed and passive force are more sensitive to this phenomenon, as proven by e.g. Ventura et al. during the machining of AISI 4140 [48]. He tested this material at two different hardness and toughness and shear stress increased as these properties increased. These properties and shear stress also increase as the temperature in the cutting zone decreases. The increasing cutting force and passive force were also measured by Hong et al. for titanium alloy cooled by LN_2 [49].

3.3.2. Tool wear

Cutting tool wear was highest for HPC 80/80 bar and lowest for HPC 160/160 (Fig. 16). The comparison of photographs revealed different tool wear progression. There was no chipping in the tool wear when HPC 40- and 60-bar were used. Higher pressures caused small fractures on the

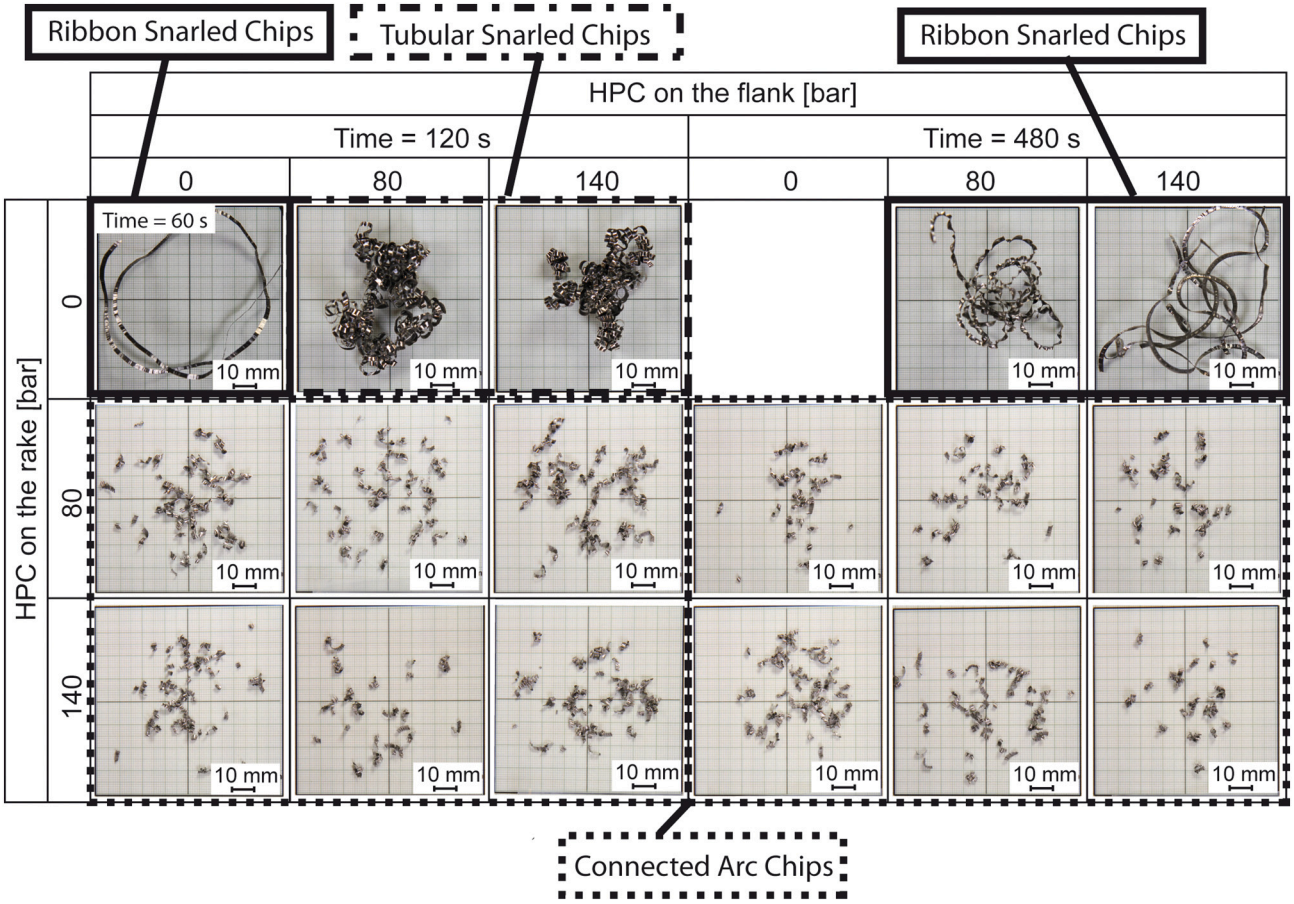

Fig. 12. Chip shape comparison for various HPC modes after 2 min and 8 min in the cut.

Table 10
ANOVA table of results for chip curl radius when various HPC modes were used.

Source	DF	Adj SS	Adj MS	F-value	*p*-Value
Time	3	0.0012	0.0012	0.80	0.401
HPC on rake	2	0.0205	0.0205	14.12	0.007
HPC on flank	1	0.0026	0.0013	0.91	0.446
Error	17	0.0102	0.0014		
Total	23	0.0345			

Table 11
ANOVA table of results for chip thickness when various HPC modes were used.

Source	DF	Adj SS	Adj MS	F-value	*p*-Value
Time	3	0.0001	0.0001	0.39	0.546
HPC on rake	2	0.0016	0.0008	6.65	0.015
HPC on flank	1	0.0001	0.0001	0.58	0.579
Error	17	0.0012	0.0001		
Total	23	0.0034			

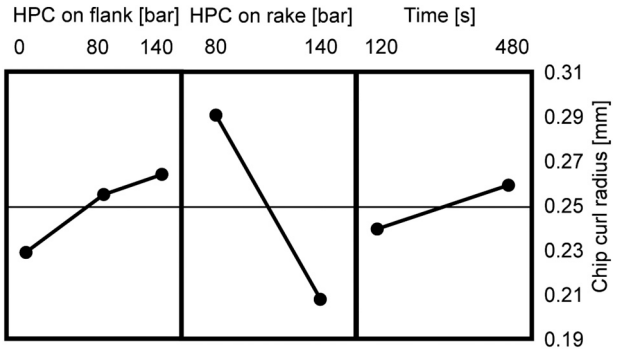

Fig. 13. Main effect plot for chip curl radius when various HPC modes were used.

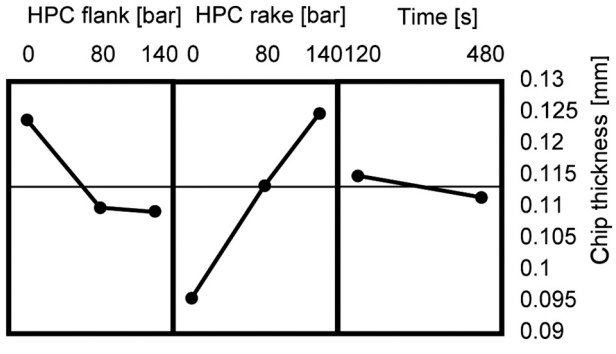

Fig. 14. Main effect plot for chip thickness when various HPC modes were used.

cutting edge. The fractures were probably caused by dynamic effects on the chip formation, which changed its form between HPC 60 to 80 bar (Fig. 21). The appearance of these fractures above 80 bar decreases with increasing HPC, most likely due to higher pressure on the back side of the chip, which reduced the negative chip formation effect of short arc chips on the cutting edge.

Analysis of variance revealed that HPC and machining time have a

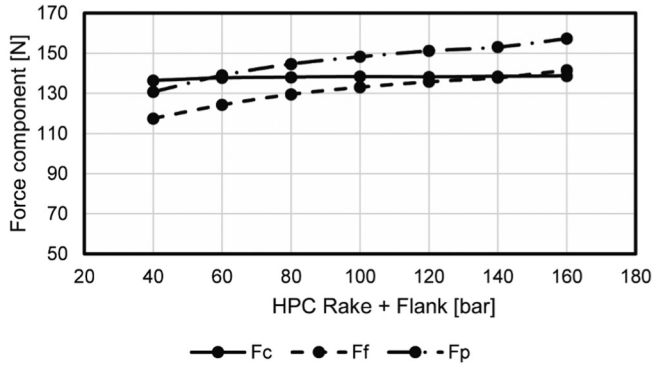

Fig. 15. Effect of coolant on force components when various HPC intensities were used

statistically significant effect on VB_c and KB at the 0.05 significance level; see Tables 12 and 13. Based on the F-value, the higher significance of the control factor time can be estimated for VB_c and KB. The coefficient of determination was 94.2 % for the VB_c model and 91.5 % for the KB model.

The main effect plot showed a decreasing dependence on HPC (Fig. 17). However, at HPC 60 bar, VB_c and KB were very small compared to 40 or 80 bar. The lowest tool wear was measured at HPC of 140 and 160 bar. Klocke also measured a decreasing flank wear trend in the range of 80 to 300 bar on gamma titanium aluminide [50]. Tool wear increased almost linearly over time, and more steeply for flank wear. Similar cutting conditions were used by Da Silva, who measured a relatively high tool life for HPC 70 bar and 110 bar when $v_c = 250$ m/min was used in comparison to 203 bar [30]. That indicates that lower HPC pressure could be more advantageous than higher pressure in some cases.

The measured point at 60 bar was very interesting in terms of reducing not only tool wear but also energy consumption during machining. The difference between 60 and 140 bar is quite significant in terms of energy consumption compared to the relatively small increase in tool life. However, the chips were carried against the unmachined surface of the workpiece at very high pressures (140 and 160 bar). The high energy of the coolant stream with chips damaged the unmachined surface by blasting and created visible scratches (Fig. 18). This is not a suitable phenomenon if the scratched surface remains unmachined. A similar issue was observed on the cutting tool. Scratches were also visible on the rake face of the cutting tool and in addition, the cutting edge was damaged by fractures due to HPC chip blasting, see Fig. 19. This decreases the overall life of the circular indexable insert because it reduces the number of possible usable cutting edges that may be created by rotating the indexable insert.

3.3.3. Surface roughness

Surface roughness measurements showed that HPC had a significant influence on this property. As mentioned above, a very high HPC intensity led to scratching of the unmachined surface, but it also increased the surface roughness on the machined surface; see Fig. 20. Machining time did not have a statistically significant effect on surface roughness; see Table 14. A determination coefficient of 76 % was calculated for this model. The increase in surface roughness with machining time correlates with [40].

3.3.4. Chips

Low HPC pressure below 80 bar formed short tubular chips. Above this limit, the chips were only arc shaped and mostly connected (Fig. 21).

Chip formation was influenced by coolant pressure. The higher the cooling pressure, the closer it gets to the cutting edge. The cooling creates hydraulic pressure which acts on the outer side of the chip and bands it; see Fig. 22a. At higher pressure, increased bending of chips can be observed. Subsequently, a smaller chip curl radius occurred; see Fig. 23. The same phenomenon was described in ref. [51] or in ref. [52]. Above HPC 60 bar, the chips were broken on the short length. As the pressure was further increased, the length of the chip did not change significantly.

Chip curl radius was significantly affected by HPC, but not by machining time (Table 15). Curl radius decreased with HPC intensity. At low HPC pressure, the curl radius was almost double because the chips had different shapes (Fig. 23).

Chip width was independent of HPC, and machining time and results are not presented for this reason.

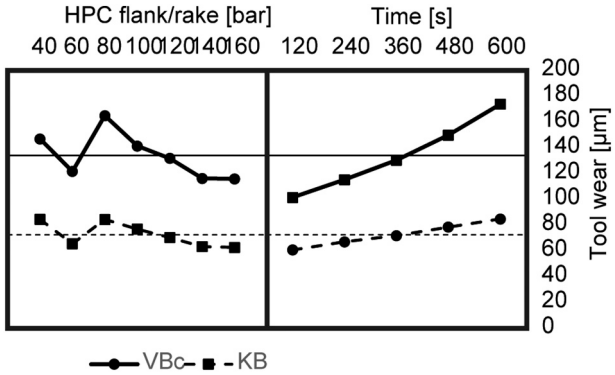

Fig. 17. Main effect plot for VB_c and KB when various HPC intensities were used.

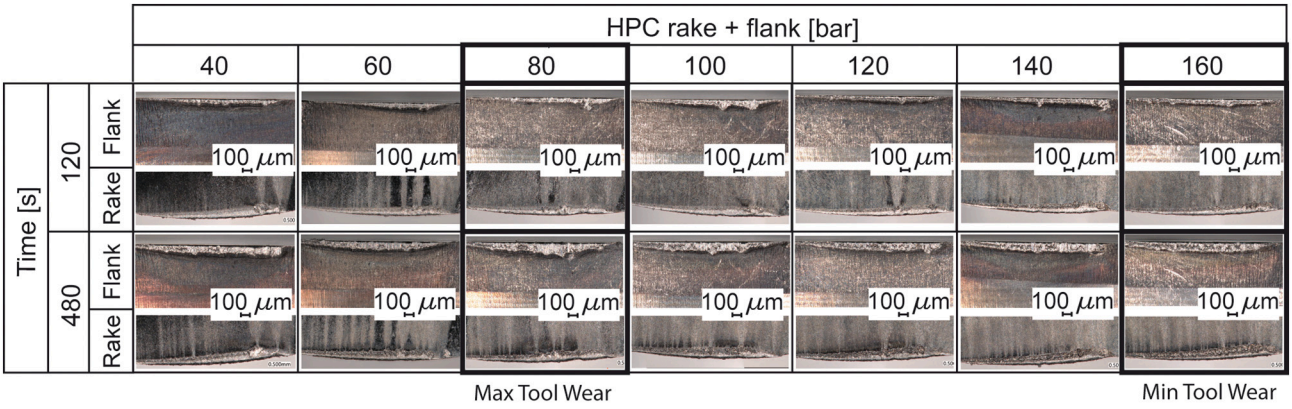

Fig. 16. Cutting tool wear comparison for various HPC intensities after 2 min and 8 min in the cut.

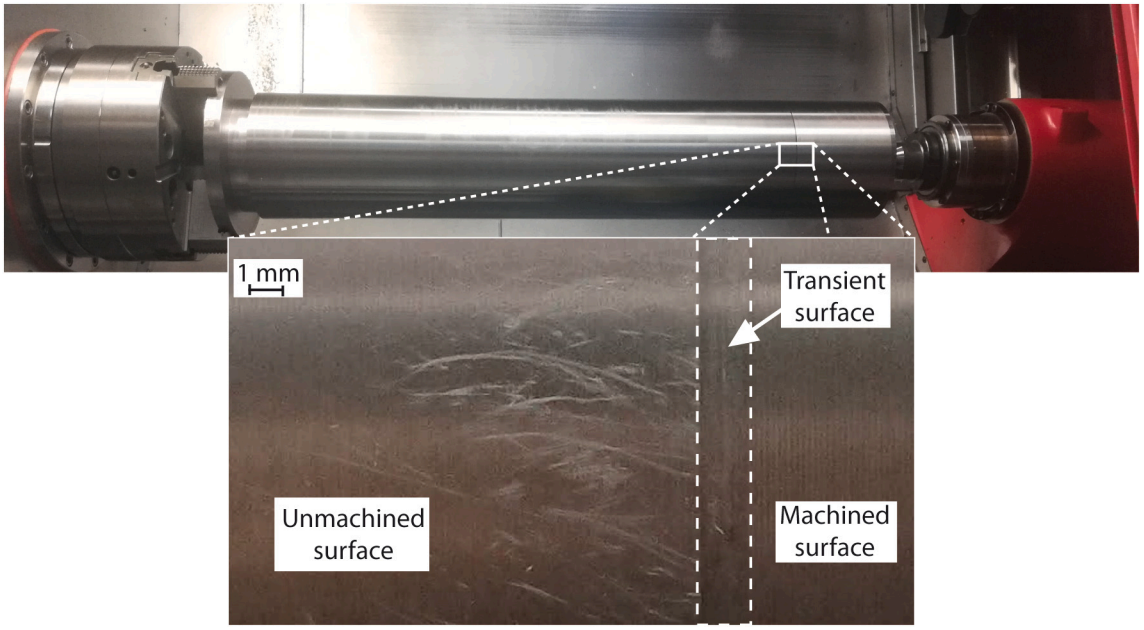

Fig. 18. Damages on the unmachined surface caused by HPC and chips under 140 bars.

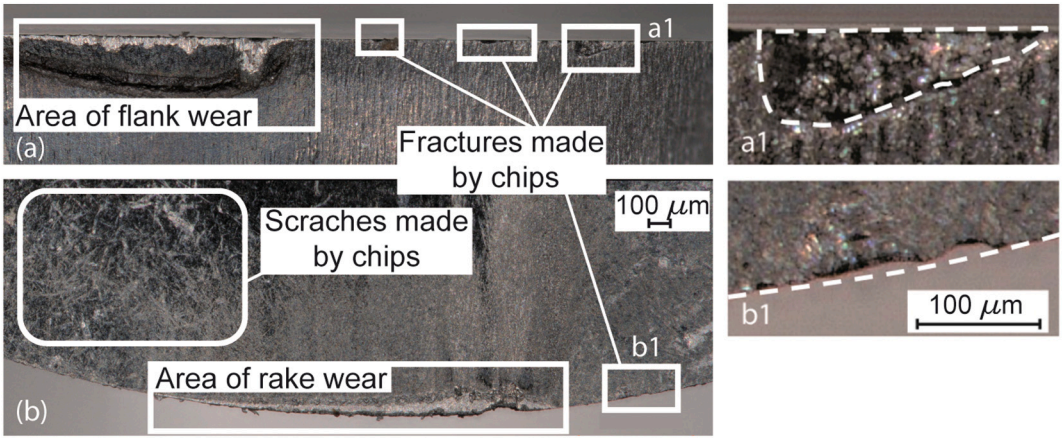

Fig. 19. Damages on the indexable insert caused by HPC and chips under 140 bars: (a) flank surface, (b) rake surface

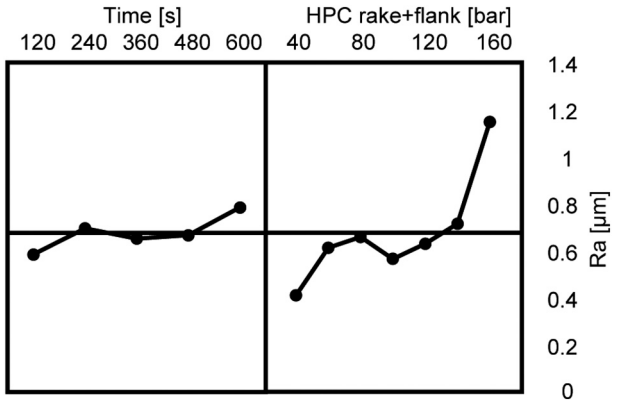

Fig. 20. Main effect plot for Ra when various HPC intensities were used.

4. Conclusions

Although PCD is not generally suitable for titanium alloy machining because of titanium alloy's low thermal conductivity, the cutting material's low thermal durability, the high reactivity of the carbon and titanium and the cutting edge's high mechanical load, there are cutting conditions which allow highly productive machining of this combination of workpiece and cutting tool material. The main results of this study are:

- A cutting speed of 300 m/min at HPC 80 bar on the rake and flank faces was suitable. A lower cutting speed caused a brittle fracture of the cutting edge. A higher cutting speed caused an excessive thermal load of the cutting edge and rapid tool wear.
- Machining without cooling was not possible at 300 m/min due to intensive thermal-induced tool wear. Tool wear was smallest when the cooling was applied from both the rake and the flank at once. HPC used only on the flank was insufficient for heat dissipation from the cutting zone. Chipping occurred when HPC was used only on the rake.

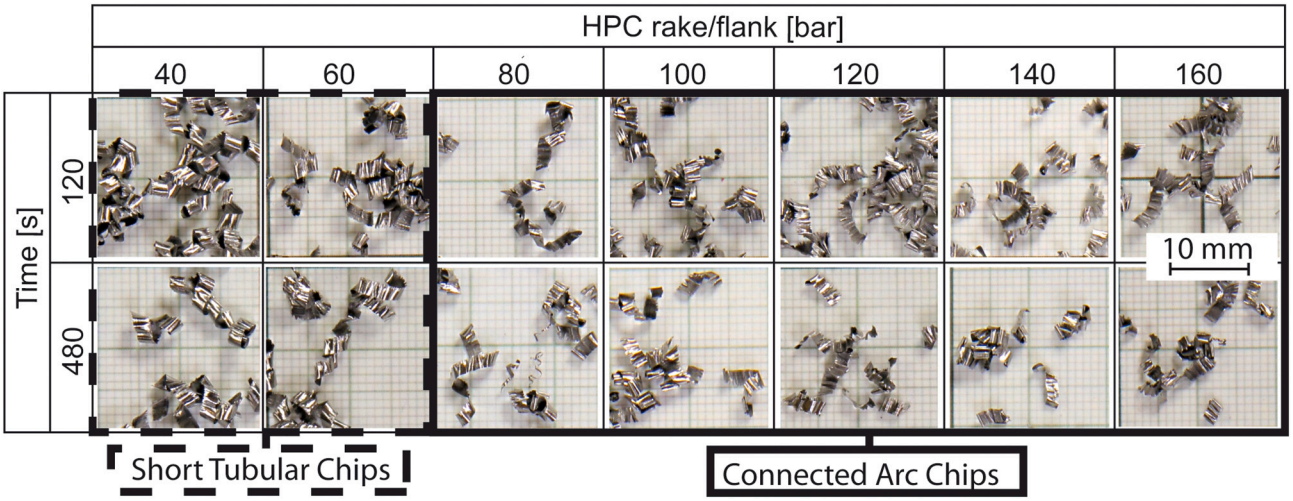

Fig. 21. Chip shape comparison for various HPC intensity levels after 2 min and 8 min in the cut.

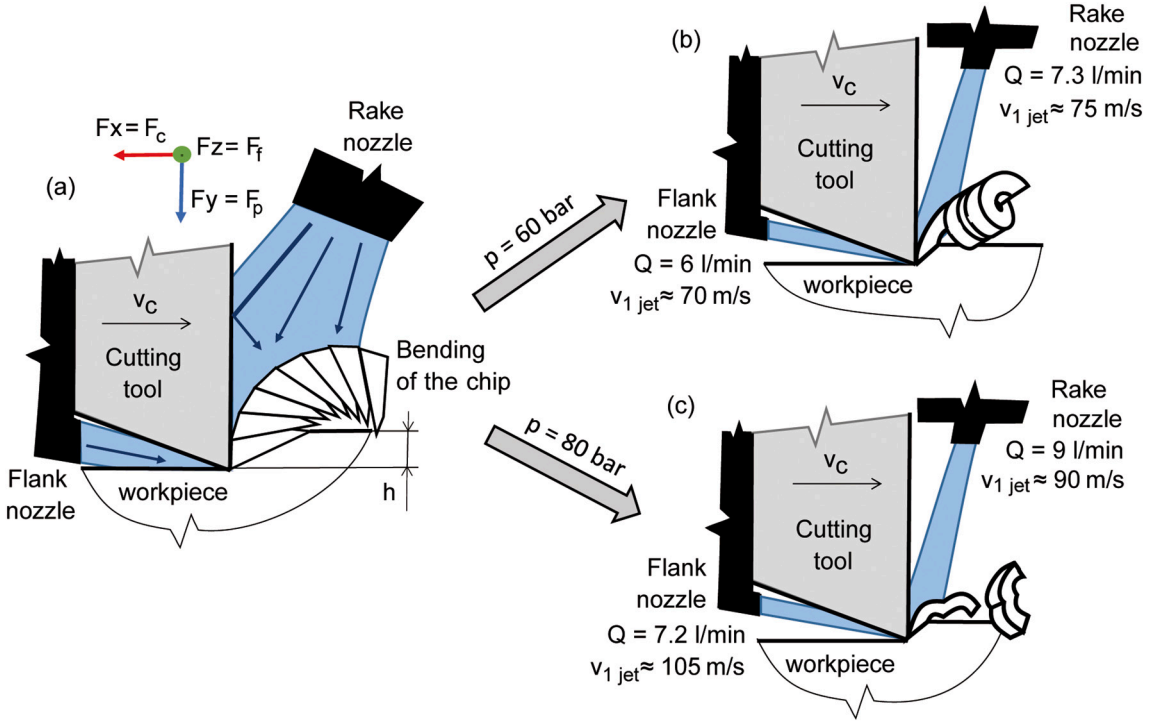

Fig. 22. Chip formation: (a) detail of the chip bending under HPC (inspired by ref. [51]), (b) small bending of the chip - short tubular chips, (c) large bending of the chip – connected arc chips.

- Investigation showed that when machining Ti alloy with a PCD tool, dual cooling is highly recommended. It is common practice to set the highest pressure available. However, the results illustrated the appropriate HPC intensity was around 60 bars at both rake and the flank. The tool wear was reduced and the cutting edge was preserved. Using the dual cooling approach at optimized pressure could be a potential solution for the industry.
- The force contribution of HPC was found. HPC acted in the feed and passive force directions. Feed and passive force increased with HPC intensity even after subtracting the force contribution of HPC.
- This is caused by enlarging of the primary cutting zone due to the cooling effect of the HPC. The passive force can affect the deflection when thin parts are turned. A lower HPC level is recommended when the presented cooling system is used for thin parts.
- Chips were mainly arc connected when HPC was applied on the rake and the pressure was above 80 bar. These types of chips caused chipping on the dynamic cutting edge behavior of chip formation. Under 80 bar pressure, short tubular chips formed. Without HPC on the rake, the chips were snarled ribbon or tubular due to heat in the cutting zone. Chip thickness and curl radius were affected mainly by HPC on the rake, where curl radius decreased with HPC intensity while chip thickness increased.
- Surface roughness increased with HPC intensity. High HPC intensity, above 140 bar, caused scratches on the unmachined surface of the workpiece, so it cannot be recommended even though tool wear was the lowest in this case.

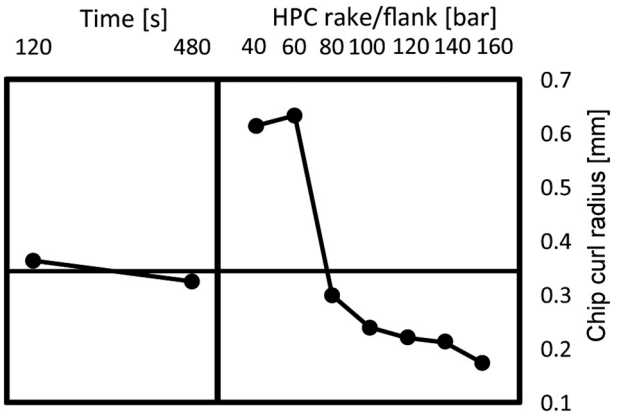

Fig. 23. Main effect plot for chip curl radius when various HPC intensities were used.

Table 12
ANOVA table of results for flank wear VB_c when various HPC intensities were used.

Source	DF	Adj SS	Adj MS	F-value	*p*-Value
HPC on rake/flank	6	9903	1650.47	19.63	0.000
Time	4	22803	5700.81	67.80	0.000
Error	24	2018	84.08		
Total	34	34724			

Table 13
ANOVA table of results for rake wear KB when various HPC intensities were used.

Source	DF	Adj SS	Adj MS	F-value	*p*-Value
HPC on rake/flank	6	2688.0	448.01	22.41	0.000
Time	4	2482.2	620.54	31.04	0.000
Error	24	479.7	19.99		
Total	34	5649.9			

Table 14
ANOVA table of results for Ra when various HPC intensities were used.

Source	DF	Adj SS	Adj MS	F-Value	*p*-Value
Time	4	0.1486	0.03716	1.64	0.198
HPC on rake/flank	6	1.5637	0.26062	11.48	0.000
Error	24	0.5449	0.02270		
Total	34	2.2572			

Table 15
ANOVA table of results for chip curl radius when various HPC intensities were used.

Source	DF	Adj SS	Adj MS	F-Value	*p*-Value
Time	1	0.0052	0.0052	0.49	0.510
HPC on flank/rake	6	0.4634	0.0772	7.22	0.015
Error	6	0.0642	0.0107		
Total	13	0.5329			

CRediT authorship contribution statement

Petr Masek: Writing – original draft, Design of experiment, Data analysis, Visualization. **Jan Maly:** Design of experiment, Methodology, Data acquisition, Data analysis. **Pavel Zeman:** Methodology, Writing – review & editing, Resources. **Petr Heinrich:** Supervision, Writing – review & editing. **Nageswaran Tamil Alagan:** Visualisation, Supervision, Writing – review & editing.

Declaration of competing interest

The authors declare that they have no known competing financial interests or personal relationships that could have appeared to influence the work reported in this paper.

Acknowledgement

The authors would like to acknowledge funding support from the Czech Ministry of Education, Youth and Sports under the project CZ.02.1.01/0.0/0.0/16_026/0008404 “Machine Tools and Precision Engineering” financed by the OP RDE (ERDF). The project is also co-financed by the European Union. Special thanks to University West, Trollhättan, Sweden for support with the high-pressure cooling unit.

References

[1] Wada T, Okayama K. “Tool wear of poly crystalline diamond in cutting Ti-6Al-4V alloy with high-pressure coolant supplied,”. 2017 8th International Conference on Mechanical and Aerospace Engineering (ICMAE) 2017:50–5. https://doi.org/10.1109/ICMAE.2017.8038616.
[2] Shalaby MA, Veldhuis SC. Some observations on flood and dry finish turning of the ti-6Al-4V aerospace alloy with carbide and PCD tools. Int. J. Adv. Manuf. Technol. Dec. 2018;99(9):2939–57. https://doi.org/10.1007/s00170-018-2675-5.
[3] Nguyen T, Kwon P, Kang D, Bieler TR. The origin of flank Wear in turning ti-6Al-4V. J. Manuf. Sci. Eng. Sep. 2016;138(12). https://doi.org/10.1115/1.4034008.
[4] Sun FJ, Qu SG, Pan YX, Li XQ, Li FL. Effects of cutting parameters on dry machining ti-6Al-4V alloy with ultra-hard tools. Int. J. Adv. Manuf. Technol. Jul. 2015;79(1):351–60. https://doi.org/10.1007/s00170-014-6717-3.
[5] Pretorius CJ, Leung Soo S, Aspinwall DK, Harden PM, M’Saoubi R, Mantle AL. Tool wear behaviour and workpiece surface integrity when turning Ti–6Al–2Sn–4Zr–6Mo with polycrystalline diamond tooling. CIRP Annals Jan. 2015;64(1):109–12. https://doi.org/10.1016/j.cirp.2015.04.058.
[6] Li G, Li N, Wen C, Ding S. Investigation and modeling of flank wear process of different PCD tools in cutting titanium alloy Ti6Al4V. Int. J. Adv. Manuf. Technol. Mar. 2018;95(1):719–33. https://doi.org/10.1007/s00170-017-1222-0.
[7] Li G, Yi S, Sun S, Ding S. Wear mechanisms and performance of abrasively ground polycrystalline diamond tools of different diamond grains in machining titanium alloy. J. Manuf. Process. Oct. 2017;29:320–31. https://doi.org/10.1016/j.jmapro.2017.08.010.
[8] Li G, Yi S, Wen C, Ding S. Wear mechanism and modeling of tribological behavior of polycrystalline diamond tools when cutting Ti6Al4V. J. Manuf. Sci. Eng. Oct. 2018;140(12). https://doi.org/10.1115/1.4041327.
[9] Priarone PC, Klocke F, Faga MG, Lung D, Settineri L. Tool life and surface integrity when turning titanium aluminides with PCD tools under conventional wet cutting and cryogenic cooling. Int. J. Adv. Manuf. Technol. 2016;1–4(85):807–16. https://doi.org/10.1007/s00170-015-7958-5.
[10] da Silva LR, da Silva OS, dos Santos FV, Duarte FJ, Veloso GV. Wear mechanisms of cutting tools in high-speed turning of Ti6Al4V alloy. Int. J. Adv. Manuf. Technol. Jul. 2019;103(1):37–48. https://doi.org/10.1007/s00170-019-03519-2.
[11] Sadik MI, Coronel E, Lattemann M. Influence of characteristic properties of PCD grades on the wear development in turning of β-titanium alloy (Ti5Al5V5Mo3Cr). Wear Apr. 2019;426–427:1594–602. https://doi.org/10.1016/j.wear.2019.01.012.
[12] Pigott RJS, Colwell AT. Hi-jet system for increasing tool life. Warrendale, PA: SAE International; Jan. 1952. https://doi.org/10.4271/520254. SAE Technical Paper 520254.
[13] Tamil Alagan N, Hoier P, Zeman P, Klement U, Beno T, Wretland A. Effects of high-pressure cooling in the flank and rake faces of WC tool on the tool wear mechanism and process conditions in turning of alloy 718. Wear Sep. 2019;vol. 434–435:102922. https://doi.org/10.1016/j.wear.2019.05.037.
[14] Machado AR, Wallbank J. The effects of a high-pressure coolant jet on machining. Proc. Inst. Mech. Eng. BJ. Eng. Manuf. Feb. 1994;208(1):29–38. https://doi.org/10.1243/PIME_PROC_1994_208_057_02.
[15] Lindeke R, Schoenig F, Khan A, Haddad J. Machining of Alpha-Beta Titanium with Ultra-High Pressure Through the Insert Lubrication Cooling. In: Transactions of the north american manufacturing research institution of sme 1991; 1991. p. 154–61. Accessed: Oct. 10, 2022. [Online]. Available:.
[16] López de Lacalle LN, Pérez-Bilbatua J, Sánchez JA, Llorente JI, Gutiérrez A, Albóniga J. Using high pressure coolant in the drilling and turning of low machinability alloys. Int. J. Adv. Manuf. Technol. Feb. 2000;16(2):85–91. https://doi.org/10.1007/s001700050012.
[17] Ezugwu EO, Da Silva RB, Bonney J, Machado ÁR. Evaluation of the performance of CBN tools when turning Ti–6Al–4V alloy with high pressure coolant supplies. Int. J. Mach Tool. Manuf. Jul. 2005;45(9):1009–14. https://doi.org/10.1016/j.ijmachtools.2004.11.027.
[18] Vosough M. “Effect of high-pressure cooling on the residual stress in Ti-alloys during machining,” [Online]. Available:. 2005. http://urn.kb.se/resolve?urn=urn:nbn:se:ltu:diva-17957. [Accessed 10 October 2022].

[19] Sorby K, Tonnessen K. High-pressure cooling of face-grooving operations in Ti6Al4V. Proc. Inst. Mech. Eng. Part B-J. Eng. Manuf. Oct. 2006;220(10):1621–7. https://doi.org/10.1243/09544054JEM474.
[20] Benedicto E, Rubio EM, Aubouy L, Sáenz-Nuño MA. Sustainable Lubrication/Cooling Systems for Efficient Turning Operations of γ-TiAl parts from the aeronautic industry. Int. J. of Precis. Eng. and Manuf.-Green Tech. May 2022. https://doi.org/10.1007/s40684-022-00435-x.
[21] Hosokawa A, Kosugi K, Ueda T. Turning characteristics of titanium alloy ti-6Al-4V with high-pressure cutting fluid. CIRP Annals Jan. 2022;71(1):81–4. https://doi.org/10.1016/j.cirp.2022.04.064.
[22] Zębala W, Struzikiewicz G, Słodki B. Reduction of power consumption by Chip breakability control in Ti6Al4V titanium alloy turning. Materials Jan. 2020;vol. 13, no. 11, Art. no. 11. https://doi.org/10.3390/ma13112642.
[23] Pereira O, Rodríguez A, Fernández-Abia AI, Barreiro J, López de Lacalle LN. Cryogenic and minimum quantity lubrication for an eco-efficiency turning of AISI 304. J. Clean. Prod. Dec. 2016;139:440–9. https://doi.org/10.1016/j.jclepro.2016.08.030.
[24] Yang Q, Wang B, Deng J, Zheng Y, Kong X. The effect of addition of MWCNT nanoparticles to CryoMQL conditions on tool wear patterns, tool life, roughness, and temperature in turning of Ti–6Al–4 V. Int. J. Adv. Manuf. Technol. Jun. 2022;120(7):5587–604. https://doi.org/10.1007/s00170-022-09101-7.
[25] Zawada-Tomkiewicz A, Żurawski Ł, Tomkiewicz D, Szafraniec F. Sustainability and tool wear of titanium alloy thread cutting in dry and cryogenic conditions. Int. J. Adv. Manuf. Technol. Jun. 2021;114(9):2767–81. https://doi.org/10.1007/s00170-021-07034-1.
[26] Airao J, Nirala CK, Bertolini R, Krolczyk GM, Khanna N. Sustainable cooling strategies to reduce tool wear, power consumption and surface roughness during ultrasonic assisted turning of ti-6Al-4V. Tribology International May 2022;169:107494. https://doi.org/10.1016/j.triboint.2022.107494.
[27] Khanna N, Shah P, de Lacalle LNL, Rodríguez A, Pereira O. In pursuit of sustainable cutting fluid strategy for machining ti-6Al-4V using life cycle analysis. Sustain Mater Technol. Sep. 2021;29:e00301. https://doi.org/10.1016/j.susmat.2021.e00301.
[28] Siju AS, Waigaonkar SD. Effects of rake surface texture geometries on the performance of single-point cutting tools in hard turning of titanium alloy. J. Manuf. Process. Sep. 2021;69:235–52. https://doi.org/10.1016/j.jmapro.2021.07.041.
[29] Jahaziel RBibeye, Krishnaraj V, Priyadarshini BGeetha. "Investigation on influence of micro-textured tool in machining of Ti-6Al-4V alloy," [Online]. Available: J. Mech Sci. Technol. 2022;36(4):1987–95. https://doi.org/10.1007/s12206-022-0334-0.
[30] da Silva RB, Machado ÁR, Ezugwu EO, Bonney J, Sales WF. Tool life and wear mechanisms in high speed machining of Ti–6Al–4V alloy with PCD tools under various coolant pressures. J. Mater Process. Technol. Aug. 2013;213(8):1459–64. https://doi.org/10.1016/j.jmatprotec.2013.03.008.
[31] Çolak O. "Optimization of Machining Performance in High-Pressure Assisted Turning of Ti6Al4V Alloy,". 2014. https://doi.org/10.5545/SV-JME.2013.1079.
[32] Ayed Y, Germain G, Ammar A, Furet B. Tool wear analysis and improvement of cutting conditions using the high-pressure water-jet assistance when machining the Ti17 titanium alloy. Precis. Eng. Oct. 2015;42:294–301. https://doi.org/10.1016/j.precisioneng.2015.06.004.
[33] Wada T. "Cutting Performance in Threading Turning and Grooving Turning of Ti-6Al-4V Alloy with a High-Pressure Coolant Supply,". 2019 IEEE 10th International Conference on Mechanical and Aerospace Engineering (ICMAE) 2019. https://doi.org/10.1109/ICMAE.2019.8880914.
[34] Palanisamy S, McDonald SD, Dargusch MS. Effects of coolant pressure on chip formation while turning Ti6Al4V alloy. Int. J. Mach Tool Manuf. Jul. 2009;49(9):739–43. https://doi.org/10.1016/j.ijmachtools.2009.02.010.
[35] Kaynak Y, Gharibi A, Yılmaz U, Köklü U, Aslantaş K. A comparison of flood cooling, minimum quantity lubrication and high pressure coolant on machining and surface integrity of titanium ti-5553 alloy. J. Manuf. Process. Aug. 2018;34:503–12. https://doi.org/10.1016/j.jmapro.2018.06.003.
[36] Rao CM, Rao SS, Herbert MA. "Influence of Modified Cutting Inserts in Machining of Ti-6Al-4V Alloy Using PCD Insert,". Materials Today: Proceedings 2018;5(9):18426–32. https://doi.org/10.1016/j.matpr.2018.06.183. Part 3.
[37] Rao CM, Sachin B, Rao SS, Herbert MA. Minimum quantity lubrication through the micro-hole textured PCD and PCBN inserts in the machining of the Ti–6Al–4V alloy. Tribology International Jan. 2021;153:106619. https://doi.org/10.1016/j.triboint.2020.106619.
[38] Sales WF, Schoop J, Jawahir IS. Tribological behavior of PCD tools during superfinishing turning of the Ti6Al4V alloy using cryogenic, hybrid and flood as lubri-coolant environments. Tribology International Oct. 2017;114:109–20. https://doi.org/10.1016/j.triboint.2017.03.038.
[39] Revankar GD, Shetty R, Rao SS, Gaitonde VN. Analysis of surface roughness and hardness in titanium alloy machining with polycrystalline diamond tool under different lubricating modes. Mat. Res. Aug. 2014;17:1010–22. https://doi.org/10.1590/1516-1439.265114.
[40] Mia M, Khan MA, Dhar NR. High-pressure coolant on flank and rake surfaces of tool in turning of ti-6Al-4V: investigations on surface roughness and tool wear. Int. J. Adv. Manuf. Technol. May 2017;90(5–8):1825–34. https://doi.org/10.1007/s00170-016-9512-5.
[41] Schrock DJ, Kang D, Bieler TR, Kwon P. Phase dependent tool Wear in turning ti-6Al-4V using polycrystalline diamond and carbide inserts. J. Manuf. Sci. Eng. Jun. 2014;136(4). https://doi.org/10.1115/1.4027674.
[42] Ezugwu E, Bonney J, Da Silva R, Cakir O. Surface integrity of finished turned Ti–6Al–4V alloy with PCD tools using conventional and high pressure coolant supplies. International Journal of Machine Tools & Manufacture - INT J MACH TOOL MANUF May 2007;47:884–91. https://doi.org/10.1016/j.ijmachtools.2006.08.005.
[43] Tamil Alagan N, Zeman P, Mara V, Beno T, Wretland A. High-pressure flank cooling and chip morphology in turning alloy 718. CIRP J. Manuf. Sci. Technol. Nov. 2021;35:659–74. https://doi.org/10.1016/j.cirpj.2021.08.012.
[44] Lindvall R, Lenrick F, Persson H, M'Saoubi R, Ståhl J-E, Bushlya V. Performance and wear mechanisms of PCD and pcBN cutting tools during machining titanium alloy Ti6Al4V. Wear Aug. 2020;454–455:203329. https://doi.org/10.1016/j.wear.2020.203329.
[45] Muhammad R, Hussain MS, Maurotto A, Siemers C, Roy A, Silberschmidt VV. Analysis of a free machining α+β titanium alloy using conventional and ultrasonically assisted turning. J. Mater Process. Technol. Apr. 2014;214(4):906–15. https://doi.org/10.1016/j.jmatprotec.2013.12.002.
[46] Hadzley M, et al. The high pressure waterjet asisted machining. World Applied Sciences Journal 21(Special Issue of Engineering and Technology) 2013;vol. 98–104. https://doi.org/10.5829/idosi.wasj.2013.21.1013.
[47] Zhang Y, Mabrouki T, Nelias D, Gong Y. FE-model for titanium alloy (Ti-6Al-4V) cutting based on the identification of limiting shear stress at tool-chip interface. Int. J. Mater Form. Mar. 2011;4(1):11–23. https://doi.org/10.1007/s12289-010-0986-7.
[48] Ventura CEH, Magalhães FC, Abrão AM, Denkena B, Breidenstein B. Performance evaluation of the edge preparation of tungsten carbide inserts applied to hard turning. Int. J. Adv. Manuf. Technol. Feb. 2021;112(11):3515–27. https://doi.org/10.1007/s00170-020-06585-z.
[49] Hong SY, Ding Y, Jeong W. Friction and cutting forces in cryogenic machining of Ti–6Al–4V. Int. J. Mach Tool Manuf. Dec. 2001;41(15):2271–85. https://doi.org/10.1016/S0890-6955(01)00029-3.
[50] Klocke F, Settineri L, Lung D, Priarone PClaudio, Arft M. "High performance cutting of gamma titanium aluminides: Influence of lubricoolant strategy on tool wear and surface integrity,". Wear 2013;302(1):1136–44. https://doi.org/10.1016/j.wear.2012.12.035.
[51] Machado AR, Wallbank J, Pashby IR, Ezugwu EO. TOOL PERFORMANCE AND CHIP CONTROL WHEN MACHINING Ti6A14V AND INCONEL 901 USING HIGH PRESSURE COOLANT SUPPLY. Machining Science and Technology Aug. 1998;2(1):1–12. https://doi.org/10.1080/10940349808945655.
[52] Polvorosa R, Suárez A, de Lacalle LNL, Cerrillo I, Wretland A, Veiga F. Tool wear on nickel alloys with different coolant pressures: comparison of alloy 718 and waspaloy. J. Manuf. Process Apr. 2017;26:44–56. https://doi.org/10.1016/j.jmapro.2017.01.012.

Petr Masek holds a PhD in Mechanical Engineering from the Czech Technical University (CTU) in Prague. Since 2011, he has been working as a researcher and lecturer at the Department of Production Machines and Equipment of the Czech Technical University. He is a specialist in the machining of composites and designing experiments in terms of machining technology. Currently, his research focuses on ultra-hard cutting tools such as boron nitride or diamond, difficult-to-cut materials, and the development of experimental machining methods. He has been involved in various collaborative projects with industries and research centres in Europe.

Jan Maly is a graduate of the Faculty of Mechanical Engineering of the Czech Technical University, where he received his master's degree in 2007. Since 2006 he has been working at the Department of Production Machines and Equipment at CTU as a researcher in the field of machining technology. Since 2012 he has been working as a professional academic, specialist in machining technology. He has participated in many research activities in cooperation with the industry, especially in testing cutting tools in terms of their tool life. His area of interest is the machining of difficult-to-machine materials.

Pavel Zeman is a senior researcher at the Research Centre for Manufacturing Technologies at the Faculty of Mechanical Engineering of the Czech Technical University in Prague. He completed his doctoral studies at this institution with a focus on the plastic deformation of materials in the cutting zone. Currently, he leads a technology group and several teams working on joint projects with the largest Czech cutting tool manufacturers and end users. His research focuses on the efficiency of machining difficult-to-cut materials for the energy and aerospace industries. He develops new solutions for cutting tools made of super-hard materials.

Petr Heinrich is a graduate of the Faculty of Mechanical Engineering of CTU. He gained a lot of experience during 9 years with the management of technical teams in Brisk Tábor and then in Magna Cartech - companies focused on the automotive industry. He was responsible for improving technological processes. Since 2013 he has been working for Kovosvit MAS, a very important manufacturer of machine tools in the Czech Republic. Currently, he works as a technical manager. He has gained a lot of experience in cooperation on projects with technical universities. He focuses on the technical design of machine tools.

Nageswaran Tamil Alagan has a PhD in Production Technology from University West, Sweden. He is currently working in the department of Innovation & Technology for Extrusion Europe at Norsk Hydro where he focuses on the Eco-machining of Al-alloys. He has extensive experience and has worked with high-pressure coolant-assisted machining of Heat Resistant Superalloys in Jet engines with the Chalmers University of Technology and GKN Aerospace Sweden. He has investigated the improvement of the interface between coolant and cutting insert through micro-texture in areas where high-temperature

gradients occur on the cutting tool. Further research activities include textured cutting tools, cryogenic cooling, and ultrasonic vibration-assisted machining.